Mathematical Model of a Vernier Gimballing Momentum Wheel Supported by Magnetic Bearings

Jiayi Li # 1*, Kai Xiao # 2, Kun Liu # 3, Eryong Hou # 4
College of Aerospace and Material Engineering, National University of Defense Technology,
Changsha, 410073, China

Abstract

Based on rotor dynamics and gyro dynamics, the mathematical model for a vernier gimballing momentum wheel supported by magnetic bearings was established to analyze the forces and torques generated by the wheel body. The static and couple unbalances of the structure are regarded as two main sources causing periodic disturbances to the stability of the system. Since the rotational speed of the rotor is high, the gyroscopic effect is also an important factor causing interference on the stability. Therefore, the effects of disturbances from above are considered to make the mathematical model be closer to the real state.

1 Introduction

A new concept for small satellites is proposed that uses active magnetic bearings to support and tilt a spinning rotor to provide 3-axis attitude control of the satellite using a single actuator. A controlled 3-axis motion of the spinning rotor generates a conventional torque about the spin axis and a gyroscopic torque in any direction in the plane orthogonal to the spinning axis. Thus a single vernier gimballing momentum wheel can provide torques about the three principal axes of the satellite, offering mass and power savings, or redundancy.

Most spacecrafts in orbit are equipped with ball bearing reaction or momentum wheels acting as actuators in their attitude control system. The wheels have been identified as one of the main sources of vibration noise due to residual unbalances, bearing imperfections, etc. Active magnetic bearings eliminate all contact between rotors and stators, preventing stiction, friction and wear especially in the vacuum of space. They also have some advantages such as higher speed and no lubrication, etc.

The main task of the attitude control actuators, which are mainly wheels, is to generate useful torques with sufficiently high bandwidth and accuracy. The use of AMBs lets the rotor be tilted through a small range of angles if strictly designed, giving it some additional properties. The AMBs allow the rotor to be tilted at a high angular rate, generating a large gyroscopic torque. Since the axis of the gyroscopic torque can be controlled, we propose a vernier gimballing momentum wheel which can provide output torques about all three axes of the spacecraft. The high bandwidth of the output torque makes it possible for the damping of periodic vibrations of the spacecraft, for example in rendezvous and docking procedures[1].

The rotor can only be tilted in a small range of angle. The range of tilt angle is restricted by the width of the airgap between the electromagnet pole face and the rotor. A large airgap reduces its magnetic flux density, increases the power consumption and decreases the stiffness of the bearing. The gyroscopic torque can only be generated for a short time because of the small tilt angle and high tilt rate, which makes the vernier gimballing momentum wheel more suitable for the damping of high frequency disturbances, or for high bandwidth small-angle maneuvers[1].

2 Mathematical Model

2.1 Forces in the Magnetic Bearings

In this momentum wheel, the wheel body including the motor rotor is supported in the radial direction by hybrid magnetic bearings, where permanent magnets generate bias flux and controllable electromagnets provide control flux to stabilize the system as can be seen in Fig.1.

*Contact Author Information: E-mail: ljy2008721@sina.com. Address: College of Aerospace and Material Engineering, National University of Defense Technology, Changsha, 410073, China. Tel: +86 731 84574194

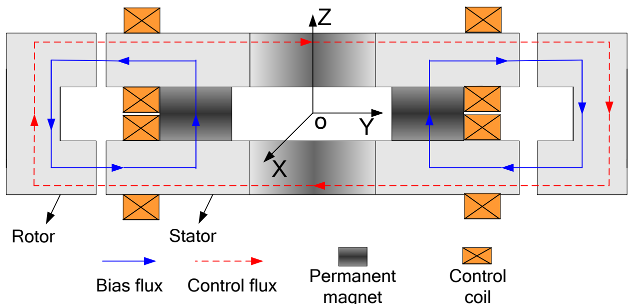

Fig.1 Flux path of the radial hybrid magnetic bearing

When the rotor is ideally suspended in the central position, the flux density of each air gap is equal to the bias flux. According to Fig.1, the resultant force in the Y direction is given by[2]

$$f = 2 \bullet \frac{(B_0 + B_i)^2 - (B_0 - B_i)^2}{2\mu_0} \bullet S_g \tag{1}$$

where B_0 is the bias flux density, B_i is the control flux density, μ_0 is the permeability of free space, and S_g is the area of pole face.

Based on the knowledge of electromagnetism, the following can be obtained:

$$\begin{cases} \Phi_g = B_0 S_g \\ E_m = \Phi_g R_g \\ E_m = H_c l_m \end{cases} \tag{2}$$

where Φ_g is the bias flux of the air gap, E_m is the magnetic motive force of the permanent magnet, R_g is the resultant reluctance, H_c is the coercive force of the permanent magnet, and l_m is the permanent magnet height in its magnetized direction.

Then the bias flux density can be derived from (2):

$$B_0 = \frac{H_c l_m}{S_g R_g} \tag{3}$$

The resultant reluctance can be calculated as

$$R_g = R_m + 2R \tag{4}$$

where R_m is the internal reluctance of the permanent magnet, and R is the reluctance of the air gap, which can be calculated as

$$\begin{cases} R = \dfrac{\delta_0}{\mu_0 S_g} \\ R_m = \dfrac{l_m}{\mu S_m} \end{cases} \tag{5}$$

where δ_0 is the length of the air gap when the rotor is suspended in the central position, μ is the permeability of the permanent magnet, and S_m is the area of the sectional area of the permanent magnet.

The electromagnetic motive force E_i can be described as follows:

$$E_i = 4ni_y \tag{6}$$

where n is the turns of each coil, and i_y is the current flowing through the coils.
Then the control flux can be expressed as

$$\Phi_i = \frac{E_i}{4R} = \frac{4ni_y}{4R} = \frac{ni_y}{R} \tag{7}$$

Therefore, the control flux density can be derived from (7):

$$B_i = \frac{\Phi_i}{S} = \frac{ni_y}{RS} \tag{8}$$

When the rotor is not suspended in the central position, the resultant force in the Y direction can be expressed as

$$f_y = 2 \bullet \frac{(B_1 + B_{i1})^2 - (B_2 - B_{i2})^2}{2\mu_0} \bullet S_g \tag{9}$$

where B_1 and B_2 are bias flux densities in the +Y and –Y directions and B_{i1} and B_{i2} are control flux densities in the +Y and –Y directions.
Similar to (3), B_1 and B_2 can be described as

$$\begin{cases} B_1 = \dfrac{H_c l_m}{S_g R_g'} \\ B_2 = \dfrac{H_c l_m}{S_g R_g''} \end{cases} \tag{10}$$

where R_g' and R_g'' are the resultant reluctances in the +Y and –Y directions respectively, which can be calculated as

$$\begin{cases} R_g' = R_m + 2R' \\ R_g'' = R_m + 2R'' \end{cases} \tag{11}$$

where R' and R'' are the reluctances of air gaps in the +Y and –Y directions, Because the rotor is not suspended in the central position, the lengths of air gaps are different in the +Y and –Y direction, which can be calculated as

$$\begin{cases} R' = \dfrac{\delta_0 + y}{\mu_0 S_g} \\ R'' = \dfrac{\delta_0 - y}{\mu_0 S_g} \end{cases} \tag{12}$$

where, y is the displacement of the rotor in the Y direction. The control flux Φ_i' can be described as

$$\Phi_i' = \frac{E_i'}{2R' + 2R''} = \frac{E_i'}{4R} \tag{13}$$

which is equal to the control flux in (7). Then the control flux density can be expressed as

$$B_{i1} = B_{i2} = \frac{ni_y'}{RS} \tag{14}$$

From (14), we can see that the control flux densities in four air gaps are equal when the rotor is not suspended in the central position.

Similar to (9), the resultant force in X direction can be expressed as

$$f_x = 2 \bullet \frac{(B_3 + B_{i3})^2 - (B_4 - B_{i4})^2}{2\mu_0} \bullet S_g \tag{15}$$

where, B_3 and B_4 are bias flux densities in the +X and –X directions which are similar to (10), and B_{i3} and B_{i4} are control flux densities in the +X and –X direction which are similar to (14).

While in the tilt magnetic bearings where ampere forces acting, permanent magnets provide a magnetic field. Actuator coils are mounted perpendicular to the magnetic field, as shown in Fig.2. An ampere force will be generated when there is current in the coils. It has the advantage of having a linear relationship between the force and the current without regard to the air gap[3]. The ampere force generated in the tilt magnetic bearing is written as follows:

$$f_{ampere} = NBIL \tag{16}$$

where N is the turns of coil in each tilt magnetic bearing, B is the magnetic induction intensity in the air gap, I is the current flowing through the coils and L is the effective length of each turn of the coil. When the currents in the two coils in the +Y and –Y directions generate the ampere forces with the same value in opposite directions, there will be a tilting torque to make the rotor tilt about the X direction.

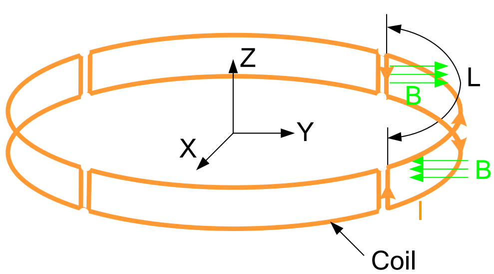

Fig. 2 The schematic diagram of the coils in the tilt magnetic bearings

2.2 Mathematical Model of the Momentum Wheel

The models of AMB flywheels supported by two-axis gimbals and single-axis gimbal have been given in [4] and [5], respectively. However, the structure of the vernier gimballing momentum wheel, as shown in Fig.3, is different from those. The schematic of the static and couple unbalance of the rotor is shown in Fig.4.

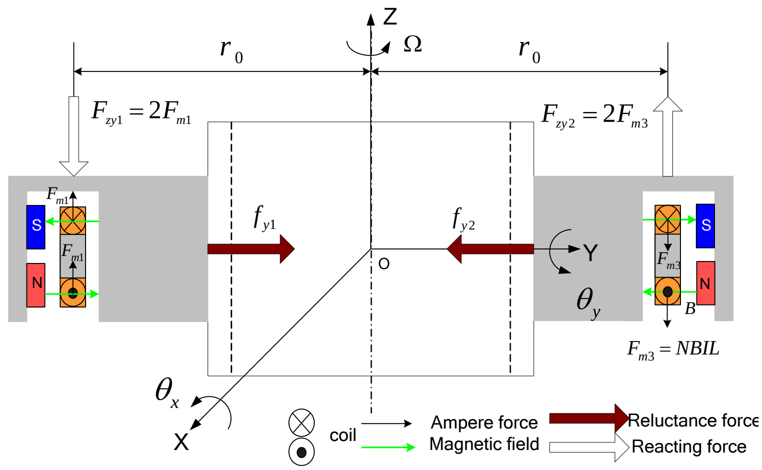

Fig.3 Sectional view of the rotor: force generation by the AMBs

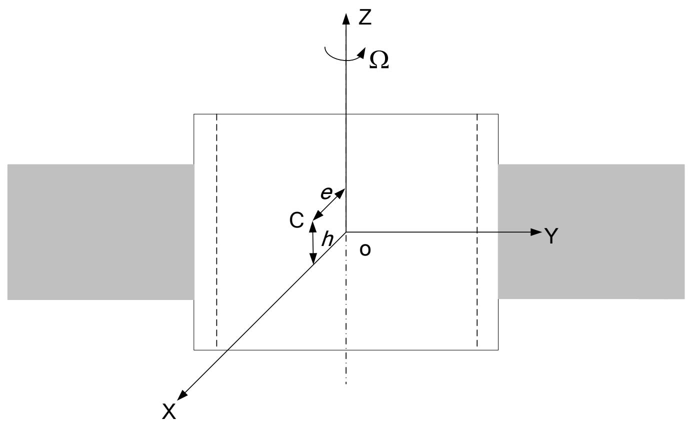

Fig.4 The static and couple unbalances of the rotor

Based on the structure given in Fig.3 and Fig.4, the symbols used in the model are listed below:

o : rotating center of the rotor

x, y : displacements of the rotor in X and Y directions, respectively

ω : rotational speed in Z direction

θ_x , θ_y : tilt angles about X and Y axes, respectively

f_{y1} , f_{y2} : reluctance forces in the Y direction

F_m : ampere force

F_{zy1} , F_{zy2} : reacting forces on the rotor

r_0 : radius of the stator where the coils of the tilt magnetic bearings mounted

C : center of mass of the rotor

e : the offset of the center of mass in the radial direction

h : the offset of the center of mass in the axial direction

As shown in Fig.4, the unbalanced force in the X and Y direction can be expressed as

$$\begin{cases} f_{dx} = M\Omega^2 e\cos\Omega t \\ f_{dy} = M\Omega^2 e\sin\Omega t \end{cases} \tag{17}$$

The unbalanced torques in X and Y direction can be described as

$$\begin{cases} T_{dx} = -f_{dy} \bullet h = -M\Omega^2 eh\sin\Omega t \\ T_{dy} = f_{dx} \bullet h = M\Omega^2 eh\cos\Omega t \end{cases} \tag{18}$$

The arms of the ampere forces are different since the coil in the tilt magnetic bearing is bended which is illustrated in Fig.5. o_1 is the center of the upper circle. P is the corner of the coil. Q is the point where ampere force element is. $F_{m1}, F_{m2}, F_{m3}, F_{m4}$ represent the ampere forces in the –Y, +X, +Y, -X directions. I_1, I_2, I_3, I_4 represent the currents in the coils in the –Y, +X, +Y, -X directions. The variables in the +Y direction can be described as

$$\begin{cases} dF_{m3} = NBI_3 \bullet r_0 d\varphi \\ \theta = 45^\circ + \varphi \\ r = r_0 \sin\varphi = r_0 \sin(45^\circ + \varphi) \end{cases} \tag{19}$$

where dF_{m3} is the ampere force element in the +Y direction, θ is the angle between the plane X-o-Z and the vector where dF_{m3} located. φ is the angle between $\overrightarrow{o_1P}$ and $\overrightarrow{o_1Q}$, and $d\varphi$ is the angle element. Then the torque element generated by the coil in the +Y direction can be expressed as

$$dT_t' = r \bullet dF_{m3} = N \bullet B \bullet I_3 \bullet r_0^2 \bullet d\varphi \bullet \sin(45^\circ + \varphi) \tag{20}$$

Therefore, the tilt torque generated by the ampere forces in the X direction can be calculated as

$$\begin{aligned} T_{tx}' &= 2 \bullet \int r \bullet dF_{m1} + 2 \bullet \int r \bullet dF_{m3} \\ &= 2 \bullet \int_0^{90^\circ} N \bullet B \bullet I_1 \bullet r_0^2 \bullet d\varphi \bullet \sin(45^\circ + \varphi) + 2 \bullet \int_0^{90^\circ} N \bullet B \bullet I_3 \bullet r_0^2 \bullet d\varphi \bullet \sin(45^\circ + \varphi) \\ &= 2\sqrt{2} N \bullet B \bullet I_1 \bullet r_0^2 + 2\sqrt{2} N \bullet B \bullet I_3 \bullet r_0^2 \\ &= 2\sqrt{2} N \bullet B \bullet r_0^2 \bullet (I_1 + I_3) \end{aligned} \tag{21}$$

The numerical value of the reacting torque on the rotor is the same as T_{tx}' which is

$$T_{tx} = T_{tx}' \tag{22}$$

Similar to the torque generated by the tilt magnetic bearings in the X direction, the torque generated by the tilt magnetic bearings in the Y direction can be shown as

$$T_{ty} = T_{ty}' = 2\sqrt{2} N \bullet B \bullet r_0^2 \bullet (I_2 + I_4) \tag{23}$$

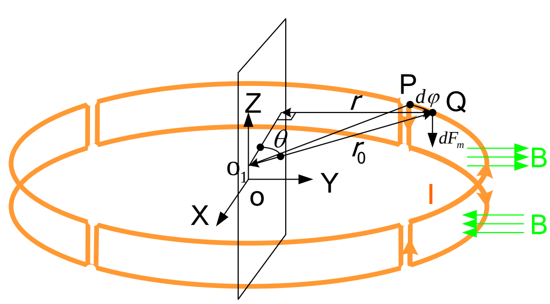

Fig.5 The arm of the ampere force

Define that $\dot{\theta}_x$ and $\dot{\theta}_y$ are the angular velocities of the rotor about the X and Y axes.

Based on the Newton's Second Law and the D'Alembert principle with (9), (15), (17), (18), (22) and (23), the mathematical model including the gyroscopic effect and the unbalanced forces (torques) is described as follows:

$$\begin{cases} M\ddot{x} = f_x + f_{dx} \\ I_y\ddot{\theta}_y = T_{ty} + I_z\Omega\dot{\theta}_x + T_{dy} \\ M\ddot{y} = f_y + f_{dy} \\ I_x\ddot{\theta}_x = T_{tx} - I_z\Omega\dot{\theta}_y + T_{dx} \end{cases} \tag{24}$$

2.3 Cylindrical and Conical Whirling of the Rotor

The static and couple unbalances can cause cylindrical and conical whirling of the rotor. Translational motion occurs with the axis of the rotor remaining parallel to itself and is referred to as cylindrical whirling; rotational motion occurs about the center of mass and is called conical whirling[6]. Table 1 shows the parameters of the momentum wheel.

Nomenclature	Value	Unit
Mass of rotor(M)	5	kg
Moment of inertia about Z axis(I_z)	0.05	kgm^2
Moment of inertia about X or Y axis($I_x = I_y = I_r$)	0.036	kgm^2
Distance from the center of gravity to the coils of tilt magnetic bearings(r_0)	100	mm
Force-displacement factor of the radial magnetic bearing (k_s)	400	kN/m
Force-current factor of the radial magnetic bearing (k_i)	120	N/A
Turns of the coil in each tilt magnetic bearing(N)	150	/
Magnetic induction intensity of the permanent magnet in the tilt magnetic bearings(B)	0.5	T
The effective length of each turn of the coil in the tilt magnetic bearings(L)	150	mm

Table 1 Parameters of momentum wheel

A PD controller has been used in this paper and the control current of the radial magnetic bearing is

$$i = \left(K_p x + K_d \dot{x}\right) G_p G_s \tag{25}$$

where, K_p and K_d are the proportional and differential coefficients of the controller. G_p and G_s are the transfer functions of power amplifier and sensor respectively.

$$G_p = \frac{0.5}{0.0003s+1} \approx 0.5$$

$$G_s = 8000$$

$$K_p = 0.85$$

The reluctance force can be described as follows(using PD controller):

$$\begin{aligned} f &= -2\left(-k_s x + k_i i\right) \\ &= -2\left(-k_s x + k_i K_p G_p G_s x + k_i K_d G_p G_s \dot{x}\right) \\ &= -\left[2\left(-k_s + k_i K_p G_p G_s\right)x + 2k_i K_d G_p G_s \dot{x}\right] \\ &= -\left(K_{11} x + C_{11}\dot{x}\right) \end{aligned} \tag{26}$$

where, $K_{11} = 2\left(-k_s + k_i K_p G_p G_s\right)$ is the stiffness coefficient, and $C_{11} = 2k_i K_d G_p G_s$ is the dumping coefficient.

With reference to Fig.5, there are two pairs of cylindrical and conical whirl curves.

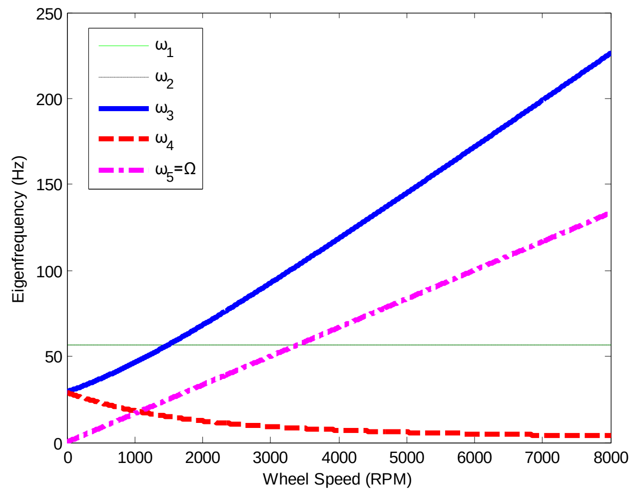

Fig.5 Campbell diagram for the rotational motions of the rotor

where, ω_1 and ω_2 are cylindrical whirl frequencies, ω_3 and ω_4 are conical whirl frequencies. ω_3 is the forward whirl frequency, which increases with the rotational speed. ω_4 is the backward whirl frequency, which decreases with the rotational speed.

3 Conclusion

This paper presented a mathematical model for the vernier gimballing momentum wheel which can help establish a suitable controller. Based on the electromagnetism, the mathematical model was derived which can also help design the active magnetic bearings. The Campbell diagram was given to analyze the cylindrical and conical whirling of the rotor. When the wheel speed comes to 1000 and 3500 RPM, the sympathetic vibration should be damped by the controller.

A conventional torque can be provided about the spin axis and a gyroscopic torque can be generated about any axis on the plane orthogonal to the spin axis. This makes it possible for the 3-axis attitude control of a spacecraft with a single momentum wheel. Thus the volume, mass and consumption of the attitude control system can be reduced.

References

[1] Jon Seddon and Alexandre Pechev. 3Dwheel: 3-Axis Low Noise, High-Bandwidth Attitude Actuation from a Single Momentum Wheel Using Magnetic Bearings. In *23rd Annual AIAA/USU Conference on Small Satellites*, 2009.

[2] Gerhard Schweitzer and Eric H. Maslen. *Magnetic Bearings: Theory, Design, and Application to Rotating Machinery*. Springer, Berlin, 2009.

[3] Bernd Gerlach, et al. Digital Controller for a Gimballing Magnetic Bearing Reaction Wheel. In *AIAA Guidance, Navigation, and Control Conference and Exhibit*, 2005.
[4] Kenta KURIYAMA, Kenzo NONAMI, and Budi RACHMANTO. Modeling and Consideration of AMB-Flywheel Supported by Two-axis Gimbals. *Journal of system design and dynamics*, **3**(4), 2009.
[5] Selim Sivrioglu. Inertial load effects on a single axis gimbal flywheel with magnetic bearings. *IEEE*, 2011.
[6] Giancarlo Genta. *Dynamics of Rotating Systems*. Springer, New York, 2005.